Available online at www.sciencedirect.com
SCIENCE DIRECT®
Journal of Organometallic Chemistry 689 (2004) 4691–4701
Journal of Organometallic Chemistry
www.elsevier.com/locate/jorganchem

Dibutyltin(IV) complexes of the 5-[(*E*)-2-(Aryl)-1-diazenyl]-2-hydroxybenzoic acid ligand: an investigation of structures by X-ray diffraction, solution and solid state tin NMR, electrospray ionisation MS and assessment of in vitro cytotoxicity

Tushar S. Basu Baul [a,*], Wandondor Rynjah [a], Rudolph Willem [b], Monique Biesemans [b], Ingrid Verbruggen [b], Michal Holèapek [c], Dick de Vos [d], Anthony Linden [e,**]

[a] *Department of Chemistry, North-Eastern Hill University, NEHU Permanent Campus, Umshing, Shillong 793 022, India*
[b] *High Resolution NMR Centre (HNMR) and Department of Polymer Science and Structural Chemistry, Vrije Universiteit Brussel (VUB), Pleinlaan 2, B-1050 Brussel, Belgium*
[c] *Department of Analytical Chemistry, University of Pardubice, Studentska 95, Pardubice, Czech Republic*
[d] *Pharmachemie BV, P.O. Box 552, 2003 RN Haarlem, The Netherlands*
[e] *Institute of Organic Chemistry, University of Zurich, Winterthurerstrasse 190, CH-8057 Zurich, Switzerland*

Received 18 May 2004; accepted 27 July 2004
Available online 8 September 2004

Abstract

A series of dibutylbis{5-[(*E*)-2-(aryl)-1-diazenyl]-2-hydroxybenzoato}tin(IV) complexes, $Bu_2Sn(LH)_2$, have been prepared and characterized by ^1H, ^{13}C, ^{119}Sn NMR and ESI mass spectrometry in solution. The structures of the complexes $Bu_2Sn(L^1H)_2$ (**1**), $Bu_2Sn(L^3H)_2$ (**3**), $Bu_2Sn(L^4H)_2$ (**4**), and $Bu_2Sn(L^6H)_2$ (**6**) (L = 5-[(*E*)-2-(aryl)-1-diazenyl]-2-hydroxybenzoate: aryl = phenyl (L^1H), 3-methylphenyl (L^3H), 4-methylphenyl (L^4H) and 4-bromophenyl (L^6H)) were determined by X-ray crystallography and ^{117}Sn CP-MAS NMR spectroscopy in the solid state. In general, the complexes were found to adopt a skew-trapezoidal bipyramidal arrangement around the tin atom. In addition, there are weak bridging intermolecular Sn···O contacts in complexes **1** and **3**, but not in **4** and **6**, where one of the hydroxy oxygen atoms from a neighboring molecule coordinates weakly with the Sn atom, thereby completing a seventh coordination site in the extended Sn coordination sphere. The Sn···O distance is 3.080(2) and 3.439(2) Å in **1** and **3**, respectively, which are significantly shorter than the sum of the van der Waals radii of the Sn and O atoms (~3.8 Å). In **1**, this Sn···O interaction links the molecules into polymeric chains. In **3**, these interactions link pairs of molecules into head-to-head dimeric units. The in vitro cytotoxicity of compound **2** indicates better results than cisplatin and etoposide against seven well characterized human tumor cell lines.

Keywords: Organotin; Carboxylates; 5-[(*E*)-2-(Aryl)-1-diazenyl]-2-hydroxybenzoic acids; NMR; ESI-MS; Crystal structure

1. Introduction

Organotin carboxylates form an important class of compounds which find many applications in chemistry and biology [1–4]. Diorganotin dicarboxylate compounds, in particular, are widely used as homogeneous

* Corresponding authors. Tel.: +91 364 2722626; fax: +91 364 2550486/2721000.
** Tel.: +41 44 635 4228; Fax: +41 44 635 6812.
E-mail addresses: basubaul@nehu.ac.in, basubaul@hotmail.com (Tushar S. Basu Baul), alinden@oci.unizh.ch (A. Linden).

0022-328X/$ - see front matter © 2004 Elsevier B.V. All rights reserved.
doi:10.1016/j.jorganchem.2004.07.050

catalysts for polyurethane and RTV silicone polymerisation and for trans esterification reactions [5,6]. Owing to these applications, the structure and mechanisms of action of these diorganotin dicarboxylates remain a matter of great interest [6–9]. Lockhart et al. [6] reported the first crystal structure of diorganotin dicarboxylate, i.e. $Me_2Sn(OAc)_2$. Subsequently, a large number of structures of diorganotin dicarboxylates, $[R_2Sn(O_2CR')_2]$, containing a variety of diorganotin moieties as well as different organic substituents have appeared and in most of the instances, the coordination geometry around the Sn atom is found to be skew-trapezoidal bipyramidal [10]. A second structural type for this general formula is found for the R = Me and R′ = C_5H_4N-*o* compounds, i.e. $[Me_2Sn(O_2CC_5H_4N\text{-}o)_2]_n$ [11]. This structural type arises because the heterocyclic N atoms bond to the Sn atoms. The Sn atom in this polymeric compound is seven coordinate.

The relatively uncomplicated structural motif for the $[R_2Sn(O_2CR')_2]$ compounds offers the opportunity to monitor the effect on the structure as the electronic nature and steric profile of the R and R′ substituents are varied. Attempts to rationalize the preference for a particular structural motif have been frustrated by a lack of systematic studies, i.e. where one of the R or R′ groups in $[R_2Sn(O_2CR')_2]$ is held constant and the other is varied. A hindrance to such analyses is the availability of suitable crystals for a range of closely related compounds, but experience has shown that good X-ray quality crystals can be obtained when carboxylate ligands based on diazenylbenzoic acid derivatives are employed. In recent systematic studies of a series of $[R_3Sn(O_2CR')]$ compounds [12] (R = Me, Et, ^{n}Bu, Ph, cHex), $[R_2Sn(O_2CR')Cl]$ compounds [13] (R = Me, ^{t}Bu and Ph), and $[R_2Sn(O_2CR')_2]$ compounds [14] (R = ^{t}Bu and Ph), the carboxylate ligand was held constant as 2-[(*E*)-2-(2-hydroxy-5-methylphenyl)-1-diazenyl]benzoic acid and the crystal structures of the complexes were correlated with other spectroscopic data. As a continuation of these studies, the present report is aimed at a systematic investigation of the structures of the dibutyltin complexes of 5-[(*E*)-2-(aryl)-1-diazenyl]-2-hydroxybenzoic acid, where the carboxylate residue (R′) is now being varied by virtue of changes to the aryl group and R is held constant as ^{n}Bu (Fig. 1). The solid state crystal structures are correlated with ^{117}Sn CP MAS NMR and ^{119}Sn Mossbauer data, while their solution behaviour was evaluated using ^{119}Sn NMR in non-coordinating solvents. The cleavage of the most labile bond in the molecule was studied using ESI mass spectroscopy. Further, organotin compounds have been reported to possess cytotoxic properties indicative of a possible antitumour effect [15,16] and, for this reason the cytotoxicity tests of a representative compound were performed.

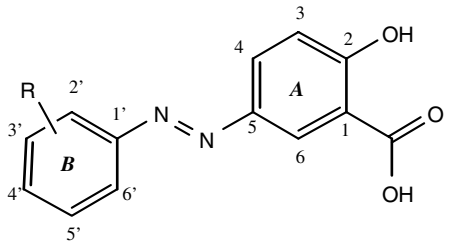

Fig. 1. Ligands used in the present work. Abbreviations: L^1HH': R = H; L^2HH': R = 2′-CH_3; L^3HH': R = 3′-CH_3; L^4HH': R = 4′-CH_3; L^5HH': R = 4′-Cl; L^6HH': R = 4′-Br, where H and H′ represent hydroxyl and carboxyl protons, respectively.

2. Experimental

2.1. Materials

Di-*n*-butyltin oxide (Fluka) was used as received. The solvents used in the reactions were of AR grade and dried using standard literature procedures.

2.2. Physical measurements

Carbon, hydrogen and nitrogen analyses were performed with a Perkin–Elmer 2400 series II instrument. IR spectra in the range 4000–400 cm^{-1} were obtained on a BOMEM DA-8 FT-IR spectrophotometer with samples investigated as KBr discs. The ^{1}H, ^{13}C and ^{119}Sn NMR spectra were recorded on a Bruker ACF 300 spectrometer and measured at 300.13, 75.47 and 111.92 MHz, respectively. The ^{1}H, ^{13}C and ^{119}Sn chemical shifts were referenced to Me_4Si set at 0.00 ppm, $CDCl_3$ set at 77.0 ppm and Me_4Sn set at 0.00 ppm, respectively. CP-MAS ^{117}Sn spectra were recorded at 89.15 MHz on a Bruker DRX250 spectrometer, equipped with a 4 or 7 mm MAS broad-band probe. The chemical shift reference was set with $(cyclo\text{-}C_6H_{11})_4Sn$ (~97.35 ppm relative to $(CH_3)_4Sn$). Solvated or unsolvated form of each compounds did not affect the NMR measurements. The positive-ion and negative-ion electrospray ionization (ESI) mass spectra were measured on unsolvated compounds using an Esquire 3000 ion trap analyzer on a Bruker Daltonics (Bremen, Germany) instrument in the range *m*/*z* 50–1000. The ion trap was tuned to give an optimum response for *m*/*z* 400. The samples were dissolved in acetonitrile and analysed by direct infusion at a flow rate of 1 μl/min. The selected precursor ions were further analysed by MS/MS and MS^n analysis under the following conditions: isolation width *m*/*z* = 8, collision amplitude 1 V, ion source temperature 300 °C, flow rate and nitrogen pressure 4 l/min and 10 psi, respectively. "Cat" means the cationic and "An" means the anionic part of the molecule [17,18] (see Section 3). The Mössbauer spectra of the complexes in the solid state were recorded using a

Model MS-900 (Ranger Scientific Co., Burleson, TX) spectrometer in the acceleration mode with a moving source geometry. A 5 mCi $Ca^{119m}SnO_3$ source was used, and counts of 30,000 or more were accumulated for each spectrum. The spectra were measured at 80 K using a liquid-nitrogen cryostat (CRYO Industries of America, Inc., Salem, NH). The velocity was calibrated at ambient temperature using a composition of $BaSnO_3$ and tin foil (splitting 2.52 mm s^{-1}). The resultant spectra were analyzed using the Web Research software package (Web Research Co., Minneapolis, MN).

2.3. Synthesis of 5-[(E)-2-(Aryl)-1-diazenyl]-2-hydroxybenzoic acids

The 5-[(*E*)-2-(Aryl)-1-diazenyl]-2-hydroxybenzoic acid ligands (L^1HH'–L^6HH') were prepared as described in earlier reports [19–22].

2.4. Synthesis of dibutylbis{5-[(E)-2-(aryl)-1-diazenyl]-2-hydroxybenzoato}tin(IV)

The dibutyltin(IV) complexes, viz., **1**–**5**, were prepared by the reaction of the appropriate LHH′ ligand with Bu_2SnO (2:1) in anhydrous benzene under reflux conditions. The steps involved in the work-up and purification are described elsewhere [19,20] while those for **6** is described below.

2.4.1. $[(L^1H)_2SnBu_2 \cdot 0.5C_6H_6]$ (1)

Orange crystals of compound **1** were obtained from benzene, mp 133–135 °C upon dissolution of $(L^1H)_2SnBu_2$ (mp 152–154 °C) [20]. Anal. Found: C, 58.82; H, 5.20; N, 7.50%. Calc. for $C_{37}H_{39}N_4O_6Sn$: C, 58.91; H, 5.21; N, 7.42%. MW = 716 was obtained on the unsolvated compound $(L^1H)_2SnBu_2$ having molecular formula $C_{34}H_{36}N_4O_6Sn$. Positive-ion MS: *m/z* 989 (100%), $[2*Cat + K]^+$; *m/z* 973, $[2*Cat + Na]^+$; *m/z* 755, $[M + K]^+$; *m/z* 738, $[M + Na]^+$; *m/z* 513, $[Cat - H + K]^+$; *m/z* 497, $[Cat - H + Na]^+$; *m/z* 475, $[Cat]^+$. Positive-ion MS/MS of 475: *m/z* 457, $[Cat - H_2O]^+$; *m/z* 431 (100%), $[Cat - CO_2]^+$; *m/z* 373, $[Cat - butane - CO_2]^+$; *m/z* 361, $[Cat - 2*butene]^+$; *m/z* 345, $[Cat - 2*butene - H_2O]^+$; *m/z* 343, $[Cat - butene - butane - H_2O]^+$; *m/z* 333, $[Cat - butene - butane - N_2]^+$; *m/z* 317, $[Cat - butene - butane - CO_2]^+$; *m/z* 299, $[Cat - butene - butane - CO_2 - H_2O]^+$; *m/z* 289, $[Cat - butene - butane - CO_2 - N_2]^+$. Negative-ion MS: *m/z* 715 (100%), $[M–H]^-$; *m/z* 241, $[An]^-$; *m/z* 197, $[An–CO_2]^-$. Negative-ion MS/MS of 715: *m/z* 241 (100%), $[An]^-$; *m/z* 197, $[An–CO_2]^-$.

2.4.2. $[(L^2H)_2SnBu_2]$ (2)

Dark-red crystals of compound **2** were obtained from a chloroform and hexane mixture, mp 120–122 °C. The analytical data and mp are in agreement with the reported values [20]. MW = 744. Positive-ion MS: *m/z* 783, $[M + K]^+$; *m/z* 767, $[M + Na]^+$; *m/z* 527, $[Cat - H + K]^+$ (100%); *m/z* 511, $[Cat - H + Na]^+$; *m/z* 489, $[Cat]^+$. Positive-ion MS/MS of 489: *m/z* 471, $[Cat - H_2O]^+$; *m/z* 445, $[Cat - CO_2]^+$; *m/z* 375, $[Cat - butene - butane]^+$; *m/z* 357, $[Cat - butene - butane - H_2O]^+$; *m/z* 347, $[Cat - butene - butane - N_2]^+$; *m/z* 331 (100%), $[Cat - butene - butane - CO_2]^+$; *m/z* 313, $[Cat - butene - butane - CO_2 - H_2O]^+$; *m/z* 303, $[Cat - butene - butane - CO_2 - N_2]^+$. Negative-ion MS: *m/z* 743 (100%), $[M–H]^-$; *m/z* 255, $[An]^-$; *m/z* 211, $[An–CO_2]^-$. Negative-ion MS/MS of 743: *m/z* 255 (100%), $[An]^-$; *m/z* 211, $[An–CO_2]^-$.

2.4.3. $[(L^3H)_2SnBu_2 \cdot 0.5C_6H_6]$ (3)

Orange crystals of compound **3** were obtained from benzene, mp 115–116 °C upon dissolution of $(L^3H)_2SnBu_2$ (mp 123–125 °C) [20]. Anal. Found: C, 59.90; H, 5.50; N, 7.20%. Calc. for $C_{39}H_{43}N_4O_6Sn$: C, 59.87; H, 5.53; N, 7.16%. MW = 744 was obtained on the unsolvated compound $(L^3H)_2SnBu_2$ having molecular formula $C_{36}H_{40}N_4O_6Sn$. Positive-ion MS: *m/z* 1001, $[2*Cat + Na]^+$; *m/z* 783, $[M + K]^+$; *m/z* 767, $[M + Na]^+$; *m/z* 527, $[Cat - H + K]^+$; *m/z* 511, $[Cat - H + Na]^+$; *m/z* 489, $[Cat]^+$ (100%). Positive-ion MS/MS of 489: *m/z* 471, $[Cat - H_2O]^+$; *m/z* 445, $[Cat - CO_2]^+$; *m/z* 387, $[Cat - butane - CO_2]^+$; *m/z* 375, $[Cat - butene - butane]^+$; *m/z* 359, $[Cat - 2*butene - H_2O]^+$; *m/z* 357, $[Cat - butene - butane - H_2O]^+$; *m/z* 347, $[Cat - butene - butane - N_2]^+$; *m/z* 331 (100%), $[Cat - butene - butane - CO_2]^+$; *m/z* 313, $[Cat - butene - butane - CO_2 - H_2O]^+$; *m/z* 303, $[Cat - butene - butane - CO_2 - N_2]^+$. Negative-ion MS: *m/z* 743 (100%), $[M–H]^-$; *m/z* 255, $[An]^-$; *m/z* 211, $[An–CO_2]^-$. Negative-ion MS/MS of 743: *m/z* 255 (100%), $[An]^-$; *m/z* 211, $[An–CO_2]^-$.

2.4.4. $[(L^4H)_2SnBu_2]$ (4)

Orange colored crystals of **4** were obtained from benzene, mp 183–185 °C upon dissolution of the yellow precipitate of $(L^4H)_2SnBu_2$ having mp 174–176 °C [20]. Anal. Found: C, 58.15; H, 5.48; N, 7.50%. Calc. for $C_{36}H_{40}N_4O_6Sn$: C, 58.09; H, 5.41; N, 7.52%. MW = 744. Positive-ion MS: *m/z* 783, $[M + K]^+$; *m/z* 767, $[M + Na]^+$; *m/z* 527, $[Cat - H + K]^+$ (100%); *m/z* 511, $[Cat - H + Na]^+$; *m/z* 489, $[Cat]^+$. Positive-ion MS/MS of 489: *m/z* 471, $[Cat - H_2O]^+$; *m/z* 445, $[Cat - CO_2]^+$; *m/z* 387, $[Cat - butane - CO_2]^+$; *m/z* 375, $[Cat - butene - butane]^+$; *m/z* 357, $[Cat - butene - butane - H_2O]^+$; *m/z* 347, $[Cat - butene - butane - N_2]^+$; *m/z* 331 (100%), $[Cat - butene - butane - CO_2]^+$; *m/z* 313, $[Cat - butene - butane - CO_2 - H_2O]^+$; *m/z* 303, $[Cat - butene - butane - CO_2 - N_2]^+$. Negative-ion MS: *m/z* 743 (100%), $[M–H]^-$; *m/z* 255, $[An]^-$; *m/z* 211, $[An–CO_2]^-$. Negative-ion MS/MS of 743: *m/z* 255 (100%), $[An]^-$; *m/z* 211, $[An–CO_2]^-$.

*2.4.5. [(L^5H)$_2$$SnBu_2$] (**5**)*

Red-orange crystals of compound **5** were obtained from benzene, mp 210–212 °C. The analytical data and mp are in agreement with the reported values [20].

*2.4.6. [(L^6H)$_2$$SnBu_2$] (**6**)*

A procedure similar to that for compounds **1**–**5** was followed [19,20]. A suspension of Bu_2SnO (0.29 g, 1.16 mmol) and L^6HH' (0.75 g, 2.33 mmol) in 50 ml anhydrous toluene were refluxed for 6 h in a flask equipped with a Dean–Stark water separator and a water cooled condenser. After the reaction, an orange colored solution was obtained and was filtered while hot. The solvent was evaporated in vacuo, the orange residue was washed thoroughly with petroleum ether (60–80 °C) and dried in vacuo. The residue was dissolved in anhydrous benzene, filtered off to remove any undissolved particles and the filtrate left to crystallize at room temperature. The orange crystals of **6** were isolated from the mother liquor and dried in vacuo. Yield: 0.81 g (79.9%), mp 180–182 °C. Anal. Found: C, 47.66; H, 3.97; N, 6.15%. Calc. for $C_{34}H_{34}N_4O_6Br_2Sn$: C, 46.77; H, 3.92; N, 6.42%. MW = 872. Positive-ion MS: no signal. Negative-ion MS: *m/z* 871 (100%), $[M–H]^-$; *m/z* 319, $[An]^-$; *m/z* 275, $[An–CO_2]^-$. Negative-ion MS/MS of 871: *m/z* 319 (100%), $[An]^-$; *m/z* 275, $[An–CO_2]^-$. ^{1}H NMR ($CDCl_3$): Ligand skeleton: 7.13 (d, 9.0 Hz, 1H, H-3), 7.66 (AA′ portion of AA′XX′, 2H, H-2′ and H-6′), 7.80 (XX′ portion of AA′XX′, 2H, H-3′ and H-5′), 8.13 (dd, 9.0 and 2.1 Hz, 1H, H-4), 8.65 (d, 2.1 Hz, 1H, H-6), 11.0 (brs, OH); Sn–Bu skeleton: 0.93 (t, 4*), 1.45 (m, 3*), 1.79 (m, 2*), 1.94 (m, 1*) ppm. ^{13}C NMR ($CDCl_3$): Ligand skeleton: 112.9 (C-1), 118.5 (C-3), 124.2 (C-2′ and C-6′), 125.1 (C-6), 128.8 (C-4), 129.0 (C-4′), 132.4 (C-3′ and C-5′), 145.4 (C-5), 151.3 (C-1′), 164.1 (C-2), 177.3 (CO_2H); Sn–Bu skeleton: 13.5 (C-4*), 26.5 (C-2*), 26.6 (C-1* and C-3*) ppm. ^{119}Sn Mössbauer spectrum: $\delta = 1.47$, $\Delta = 3.47$, $\Gamma_1\pm$ and $\Gamma_2\pm = 1.0$ mm s^{-1}, C–Sn–C = 144°.

2.5. X-ray crystallography

Crystals of compounds **1**, **3**, **4**, and **6** suitable for an X-ray crystal-structure determination were obtained from benzene (benzene/methanol for **6**). All measurments were made at low temperature on a Nonius KappaCCD diffractometer [23] with graphite-monochromated Mo Kα radiation ($\lambda = 0.71073$ Å) and an Oxford Cryosystems Cryostream 700 cooler. Data reduction was performed with HKL Denzo and Scalepack [24]. The intensities were corrected for *Lorentz* and polarization effects, and an empirical absorption

Table 1
Crystallographic data for compounds **1**, **3**, **4** and **6**

	Compound **1**	Compound **3**	Compound **4**	Compound **6**
Empirical formula	$C_{34}H_{36}N_4O_6Sn \cdot 0.5(C_6H_6)$	$C_{36}H_{40}N_4O_6Sn \cdot 0.5(C_6H_6)$	$C_{36}H_{40}N_4O_6Sn$	$C_{34}H_{34}Br_2N_4O_6Sn$
Formula weight	754.34	782.39	744.33	873.07
Crystal size (mm)	0.12 × 0.15 × 0.30	0.12 × 0.15 × 0.20	0.02 × 0.17 × 0.25	0.10 × 0.15 × 0.20
Crystal shape	Prism	Prism	Plate	Prism
Temperature (K)	160(1)	160(1)	160(1)	160(1)
Crystal system	Monoclinic	Monoclinic	Triclinic	Triclinic
Space group	$P2_1/c$	$P2_1/c$	$P\bar{1}$	$P\bar{1}$
a (Å)	11.6044(1)	9.3399(1)	9.8270(2)	9.6410(1)
b (Å)	11.5675(1)	25.1934(2)	12.1642(3)	12.1897(2)
c (Å)	25.9005(3)	15.4687(2)	14.9382(3)	15.1748(2)
α (°)	90	90	93.357(1)	94.1325(7)
β (°)	97.3428(4)	94.1425(3)	100.016(1)	98.7581(7)
γ (°)	90	90	103.805(1)	103.6085(5)
V (Å^3)	3448.21(6)	3630.34(7)	1698.29(7)	1702.24(4)
Z	4	4	2	2
D_x (g cm^{-3})	1.453	1.431	1.453	1.703
μ (mm^{-1})	0.792	0.755	0.803	3.155
Transmission factors (min, max)	0.803, 0.915	0.849, 0.917	0.903, 0.985	0.511, 0.803
$2\theta_{max}$ (°)	55	60	55	60
Reflections measured	68425	89089	36403	50202
Independent reflections (R_{int})	7888 (0.073)	10579 (0.070)	7709 (0.057)	9959 (0.057)
Reflections with $I > 2\sigma(I)$	5844	7270	6614	7455
Number of parameters	593	613	495	435
Number of restraints	660	618	134	0
$R(F)$ ($I > 2\sigma(I)$ reflns)	0.039	0.035	0.033	0.034
$wR(F^2)$ (all data)	0.091	0.087	0.077	0.076
GOF(F^2)	1.06	1.04	1.08	1.02
max, min Δρ (e/Å^3)	0.47, −0.82	1.00, −0.65	0.81, −0.68	0.77, −0.68

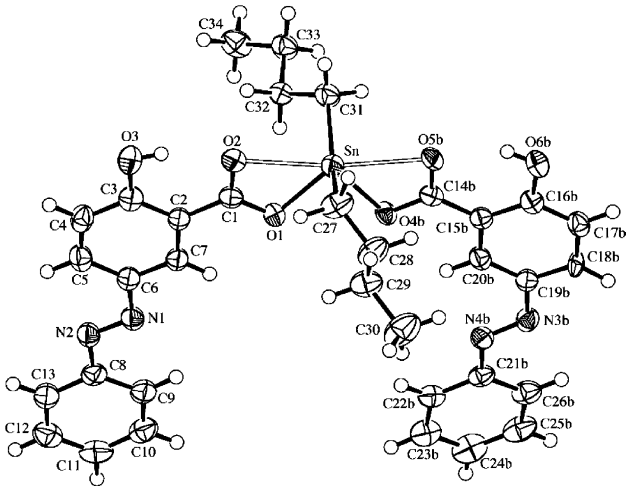

Fig. 2. The molecular structure of the major disordered conformation of **1** with the atom-labelling scheme (50% probability ellipsoids). This corresponds approximately with the minor conformation of **2**. Solvent molecule omitted.

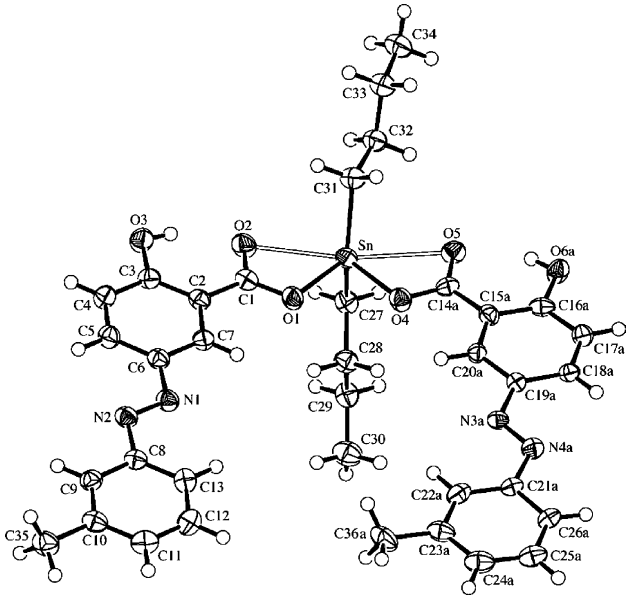

Fig. 3. The molecular structure of the major disordered conformation of **3** with the atom-labelling scheme (50% probability ellipsoids). This corresponds approximately with the minor conformation of **1**. Solvent molecule omitted.

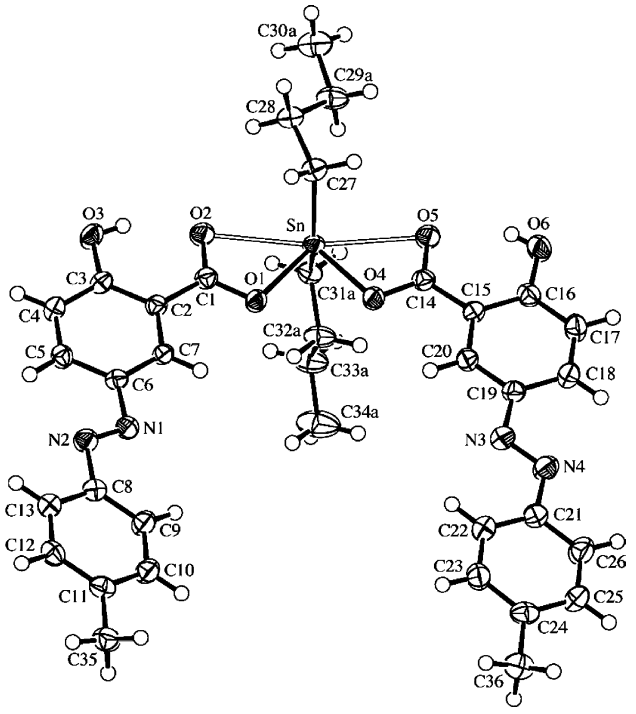

Fig. 4. The molecular structure of the major disordered conformation of **4** with the atom-labelling scheme (50% probability ellipsoids).

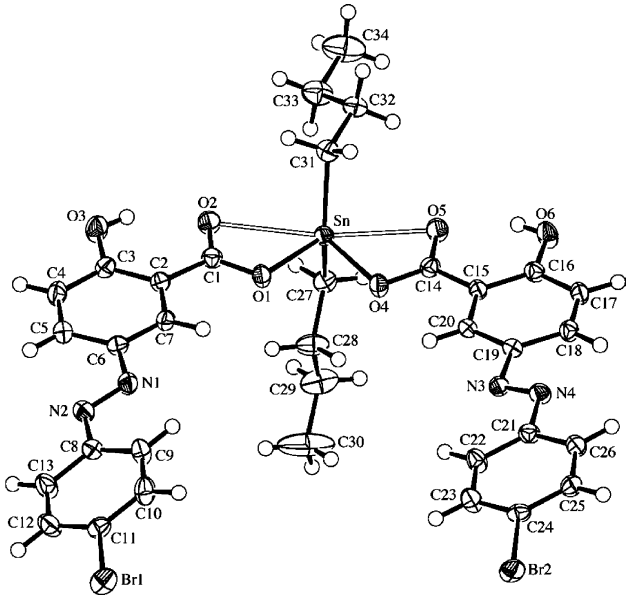

Fig. 5. The molecular structure of **6** with the atom-labelling scheme (50% probability ellipsoids).

correction based on the multi-scan method [25] was applied. Equivalent reflections were merged. The data collection and refinement parameters are given in Table 1, and views of the molecules are shown in Figs. 2–5. The structures of **1**, **3** and **4** were solved by direct methods using SIR92 [26], while that of **6** was solved by employing heavy-atom Patterson methods [27] followed by the Fourier expansion routine of DIRDIF94 [28]. In each structure, the non-hydrogen atoms were refined anisotropically, while employing restraints when necessary as described below.

For both **1** and **3**, the asymmetric unit contains one molecule of the Sn-complex, plus one half of a benzene molecule that sits about a crystallographic centre of inversion. One of the carboxylate ligands is disordered in its entirety over two conformations. Two

positions were defined for all atoms of this ligand, except for the carboxylate oxygen atoms of **3**, which are not distingushably disordered. Refinement of constrained site occupation factors for the two orientations yielded values of 0.712(6) and 0.579(5) for the major conformations of **1** and **3**, respectively. Similarity restraints were applied to the chemically equivalent bond lengths and angles of all atoms in the carboxylate ligands, including those of the ordered ligand. In this way, the well-defined geometry of the ordered ligand helped to maintain reasonable geometry within the two conformations of the disordered ligand. Furthermore, neighboring atoms within and between each conformation of the disordered ligand were restrained to have similar atomic displacement parameters. The two positions for atom C(15) in **1** were less than 0.1 Å from each other and their positions and atomic displacement parameters were ultimately constrained to be identical. The terminal phenyl ring in each of the disordered ligand conformations of **1** was also restrained to be a planar group.

For **4**, all atoms of one butyl group and the outer ethyl moiety of the other butyl group are disordered over two conformations. Refinement of constrained site occupation factors for the two orientations yielded values of 0.78(2) and 0.50(5) for the respective major conformations. Similarity restraints were applied to the chemically equivalent bond lengths and angles involving disordered C-atoms, while neighboring atoms within and between each conformation of the disordered groups were restrained to have similar atomic displacement parameters.

The H atoms of the ordered hydroxy groups in **1** and **3**, as well as those of the hydroxy groups in **4** and **6** were placed in the positions indicated by difference electron density maps and their positions were allowed to refine together with individual isotropic displacement parameters. All remaining H atoms in the structures were placed in geometrically calculated positions and refined using a riding model where each H atom was assigned a fixed isotropic displacement parameter with a value equal to $1.2U_{eq}$ of its parent atom ($1.5U_{eq}$ for the methyl and disordered hydroxy groups). The Refinement of each structure was carried out on F^2 using full-matrix least-squares procedures, which minimized the function $\sum w(F_o^2 - F_c^2)^2$. A correction for secondary extinction was applied for **4** and **6**. One, six, and seven reflections for **1**, **3**, and **6**, respectively, whose intensities were considered to be extreme outliers, were omitted from the final refinement. All calculations were performed using the SHELXL97 program [29].

2.6. Biological tests

The in vitro cytotoxicity test of compound **2** was performed using the SRB test for the estimation of cell viability. The cell lines WIDR (colon cancer), M19 MEL (melanoma), A498 (renal cancer), IGROV (ovarian cancer) and H226 (non-small cell lung cancer) belong to the currently used anticancer screening panel of the National Cancer Institute, USA [30]. The MCF7 (breast cancer) cell line is estrogen receptor (ER)+/progesterone receptor (PgR)+ and the cell line EVSA-T (breast cancer) is (ER)−/(Pgr)−. Prior to the experiments, a mycoplasma test was carried out on all cell lines and found to be negative. All cell lines were maintained in a continuous logarithmic culture in RPMI 1640 medium with Hepes and phenol red. The medium was supplemented with 10% FCS, penicillin 100 μg/ml and streptomycin 100 μg/ml. The cells were mildly trypsinized for passage and for use in the experiments. RPMI and FCS were obtained from Life technologies (Paisley, Scotland). SRB, DMSO, Penicillin and streptomycin were obtained from Sigma (St. Louis MO, USA), TCA and acetic acid from Baker BV (Deventer, NL) and PBS from NPBI BV (Emmer-Compascuum, NL).

The test compound **2** and reference compounds were dissolved to a concentration of 250,000 ng/ml in full medium, by 20-fold dilution of a stock solution which contained 1 mg of compound **2**/200 μl. Compound **2** was dissolved in DMSO. Cytotoxicity was estimated by the microculture sulforhodamine B (SRB) test [31].

2.6.1. Experimental protocol and cytotoxicity tests

The experiment was started on day 0. On day 0, 150 μl of trypsinized tumor cells (1500–2000 cells/well) were plated in 96-wells flat-bottomed microtiter plates (falcon 3072, BD). The plates were preincubated for 48 h at 37 °C, 8.5% CO_2 to allow the cells to adhere. On day 2, a three-fold dilution sequence of ten steps was made in full medium, starting with the 250,000 ng/ml stock solution. Every dilution was used in quadruplicate by adding 50 μl to a column of four wells. This results in a highest concentration of 62,500 ng/ml being present in column 12. Column 2 was used for the blank. To column 1, PBS was added to diminish interfering evaporation. On day 7, washing the plate twice with PBS terminated the incubation. Subsequently, the cells were fixed with 10% trichloroacetic acid in PBS and placed at 4 °C for an hour. After five washings with tap water, the cells were stained for at least 15 min with 0.4% SRB dissolved in 1% acetic acid. After staining, the cells were washed with 1% acetic acid to remove the unbound stain. The plates were air-dried and the bound stain was dissolved in 150 μl (10 mM) tris-base. The absorbance was read at 540 nm using an automated microplate reader (Labsystems Multiskan MS). Data were used for construction of concentration–response curves and the determination of ID_{50} values by use of Deltasoft 3 software.

3. Results and discussion

3.1. Syntheses

Treatment of Bu_2SnO with LHH′ (1:2) in toluene yielded the dibutylbis{5-[(*E*)-2-(aryl)-1-diazenyl]-2-hydroxybenzoato}tin(IV) complexes. A typical reaction is described in Section 2, along with the physical and analytical data of the complexes. The complexes are colored crystalline solids soluble in chloroform, dichloromethane, methanol, ethanol, acetonitrile, benzene, toluene and DMSO.

3.2. X-ray crystallography

The molecular structures of compounds **1**, **3**, **4**, and **6** are depicted in Figs. 2–5, respectively, while selected geometric parameters are given in Table 2. The asymmetric unit in **1** and **3** contains one molecule of the Sn-complex, plus one half of a benzene molecule. In addition, one of the carboxylate ligands in each of these structures is disordered over two conformations which arise from a reversal of the direction of the zig–zag at the N═N bond. In **1**, the major conformation is such that the C–N═N–C step points in the same direction in each ligand (Fig. 2) and is present in about 71% of the molecules. In contrast, this arrangement corresponds with the minor conformation (42%) in **3**. The alternate conformation in both structures has the C–N═N–C steps in the molecule pointing in opposite directions (Fig. 3). In **4**, both of the butyl groups are disordered, with two conformations being present for all atoms of one group and the terminal ethyl moiety of the other group. There is neither disorder nor solvent molecules in the structure of **6**.

In general, when only the primary coordination sphere is considered, all four complexes adopt the same structural motif and reveal a monomeric molecule. The carboxylate groups on the ligands act as bidentate chelating agents, giving an equatorial plane around the tin atom of four asymmetrically coordinated oxygen atoms. The carboxylate oxygen atom of each ligand

Table 2
Selected bond lengths (Å), angles (°), and torsion angles (°) for compounds **1**, **3**, **4** and **6**[a]

	Compound **1**	Compound **3**	Compound **4**	Compound **6**
Sn–O(1)	2.128(2)	2.097(1)	2.094(2)	2.082(2)
Sn–O(2)	2.512(2)	2.610(2)	2.628(2)	2.704(2)
Sn–O(4)	1.98(2), 2.178(8)	2.094(1)	2.088(2)	2.089(2)
Sn–O(5)	2.81(2), 2.490(6)	2.712(1)	2.684(2)	2.634(2)
Sn–C(27)	2.112(3)	2.117(2)	2.119(3)	2.118(2)
Sn–C(31)	2.131(3)	2.119(2)	2.122(3), 2.119(9)	2.125(2)
O(1)–C(1)	1.284(3)	1.292(2)	1.299(3)	1.294(3)
O(2)–C(1)	1.265(3)	1.259(2)	1.253(3)	1.249(3)
O(4)–C(14)	1.29(1), 1.287(6)	1.292(3), 1.298(4)	1.296(3)	1.295(3)
O(5)–C(14)	1.26(1), 1.265(6)	1.249(3), 1.256(4)	1.250(3)	1.259(3)
O(1)–Sn–O(2)	55.94(7)	54.32(5)	54.22(5)	52.97(6)
O(1)–Sn–O(4)	88.3(5), 81.3(2)	81.32(5)	82.19(6)	81.84(6)
O(1)–Sn–O(5)	140.0(4), 137.0(2)	134.00(5)	135.39(5)	135.50(6)
O(1)–Sn–C(27)	100.0(1)	104.34(7)	106.41(8)	105.14(8)
O(1)–Sn–C(31)	100.8(1)	109.61(7)	101.5(3), 106(1)	104.08(8)
O(2)–Sn–O(4)	144.3(5), 137.2(2)	135.41(5)	136.14(5)	134.79(5)
O(2)–Sn–O(5)	163.8(4), 166.6(2)	169.78(4)	170.00(5)	170.06(5)
O(2)–Sn–C(27)	85.3(1)	93.36(7)	85.51(8)	90.22(8)
O(2)–Sn–C(31)	89.56(9)	87.96(7)	89.9(4), 92(2)	87.76(8)
O(4)–Sn–O(5)	51.8(5), 55.9(2)	52.75(4)	53.21(5)	54.15(5)
O(4)–Sn–C(27)	103(1), 103.6(4)	102.75(7)	104.72(8)	102.05(8)
O(4)–Sn–C(31)	98(1), 99.6(4)	104.91(7)	104.9(3), 105(1)	106.44(8)
O(5)–Sn–C(27)	87.7(6), 88.2(3)	89.81(7)	88.16(8)	91.58(8)
C(5)–Sn–C(31)	89.4(6), 90.4(3)	83.26(7)	90.3(4), 87(2)	84.75(8)
C(27)–Sn–C(31)	150.8(1)	138.72(8)	141.5(2), 138.5(7)	141.50(9)
C(1)–O(1)–Sn	100.9(2)	105.0(1)	105.0(1)	107.4(1)
C(1)–O(2)–Sn	83.6(2)	81.8(1)	81.3(1)	79.3(1)
C(14)–O(4)–Sn	113(1), 99.2(5)	107.3(2), 107.9(2)	106.9(1)	105.4(1)
C(14)–O(5)–Sn	74.4(8), 85.4(4)	79.3(2), 79.9(2)	80.1(1)	80.9(1)
N(1)–N(2)–C(8)–C(9)	−1.9(4)	−178.2(2)	−0.1(4)	9.3(3)
N(2)–N(1)–C(6)–C(5)	−0.3(4)	0.6(3)	−15.0(3)	9.7(3)
N(3)–N(4)–C(21)–C(22)	0(1), −179.9(4)	2(1), 176(1)	−3.5(4)	−4.0(3)
N(4)–N(3)–C(19)–C(18)	−4(3), 169.7(6)	−3(1), −175(1)	−6.5(4)	12.7(3)

[a] Entries with two values correspond to disordered conformations *A* and *B* in the structure.

coordinates strongly to the Sn atom (Sn–O is in the range 1.98–2.18 Å (Table 2), although the range may be somewhat exaggerated because of the difficulty treating the disorder in **1**; excluding **1**, the range is tightly restricted to 2.09–2.10 Å), while the carbonyl oxygen atom is much more weakly bound (Sn–O is in the range 2.49–2.81 Å, or 2.61–2.71 excluding **1**). The coordination is such that the strongly bound oxygen atoms lie *cis* to one another with a very acute O–Sn–O angle (range 81–88°), while the weakly bound oxygen atoms lie only 10–16° from being linearly disposed to one another, thereby leaving one side of the Sn atom quite open. The butyl groups lie in axial positions, thereby completing six-coordination about the Sn atom, but they are distorted some 29–42° from a true *trans* position, being pinned back somewhat over the open space left by the equatorial ligands to produce a skew-trapezoidal bipyramidal structure. These observations are in excellent agreement with the coordination geometry determined from ^{119}Sn Mössbauer results [20]. These structures conform to the predominant motifs found for compounds with the general formula $[R_2Sn(O_2CR')_2]$ [10], where asymmetrically coordinated carboxylate oxygen atoms are present, with the shorter of the Sn–O bonds being $\leqslant$2.2 Å, the longer Sn–O bonds being $\geqslant$ 2.5 Å, and the two organo substituents being disposed over the longer Sn–O vectors with C–Sn–C angles in the range 130–150°. The same structural motifs were also found for recently reported structures involving cognate ligand systems [19,20].

In the structures of **1** and **3**, the open side of the Sn atom actually allows one of the hydroxy oxygen atoms from the 2-hydroxybenzoate moiety of one ligand of a neighboring molecule to form a bridge and coordinate very weakly with the Sn atom, thereby completing a seventh coordination site in the extended Sn coordination sphere. In **1**, The Sn···O distance is 3.080(2) Å, which is about 0.70 Å shorter than the sum of the van der Waals radii of the Sn and O atoms, so the interaction is significant. This bridging Sn···O interaction links the molecules into a one-dimensional polymeric structure with extended zig–zag chains running parallel to the crystallographic *b*-axis (Fig. 6). The bridging Sn···O distance in **3** is somewhat longer at 3.439(2) Å, but this is still significantly shorter than the sum of the van der Waals radii of the atoms involved, and these interactions link pairs of the molecules via two concomitant bridging interactions into head-to-head dimeric units (Fig. 7). In the structures of **4** and **6**, as in the 4-chlorophenyl analogue [20], there are no weak intermolecular Sn···O interactions. The arrangement of the butyl groups in these latter three structures is such that one butyl group extends perpendicular to the plane of the carboxylate ligands, while the other butyl group bends so that it is mainly antiparallel to the carboxylate ligands, thereby closing off access to the open side of the Sn atom. In contrast, both butyl groups in **1** and **3** extend essentially perpendicular to the plane of the carboxylate ligands like open arms, thereby leaving access open for the additional coordination.

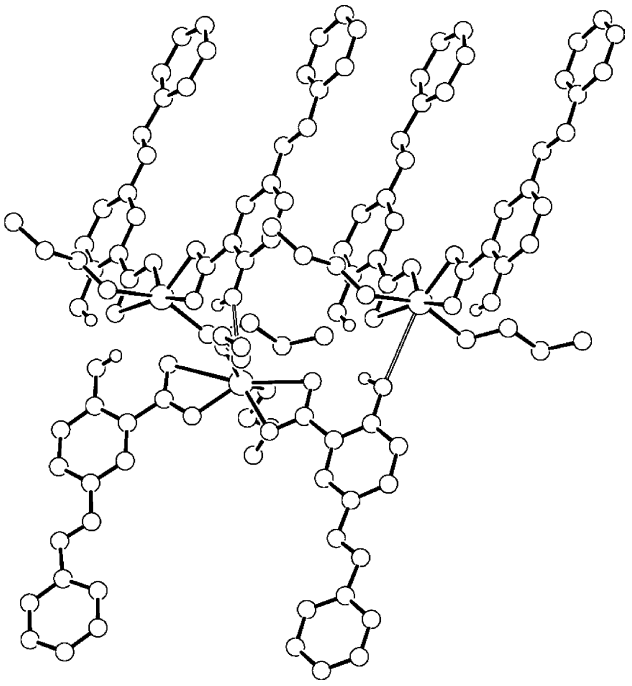

Fig. 6. Three segments of the chain structure formed by the weak Sn···O interaction (open bonds) in **1**. Except for the hydroxy groups, the hydrogen atoms have been omitted for clarity.

In **1** and **3**, the carboxylate ligands are almost completely planar and coplanar with one another. In **4** and **6**, the 2-hydroxybenzoate moieties are planar and almost coplanar with one another, but small twists about the C–N bonds result in the 4-methylphenyl groups in **4** being twisted from the planes of their associated 2-hydroxybenzoate moieties by about 10 and 15°, while in **6**, the corresponding twists of the 4-bromophenyl groups are approximately 9° and 19°.

In each structure, each 2-hydroxybenzoate hydroxy group forms an intramolecular hydrogen bond with the carboxylate carbonyl oxygen atom of the same ligand. In complexes **1** and **3**, the hydroxy oxygen atom involved in the bridging Sn···O interaction may also make a very weak intermolecular hydrogen bond with the carboxylate carbonyl oxygen atom in the other ligand of the molecule across the bridge, although this could merely be a consequence of the proximity of the respective neighboring groups caused by the intermolecular Sn···O interaction.

3.3. Mass spectrometry

The typical feature of the ESI mass spectra of organotin compounds is the cleavage of the most labile bond in the molecule to yield two complementary ions, where

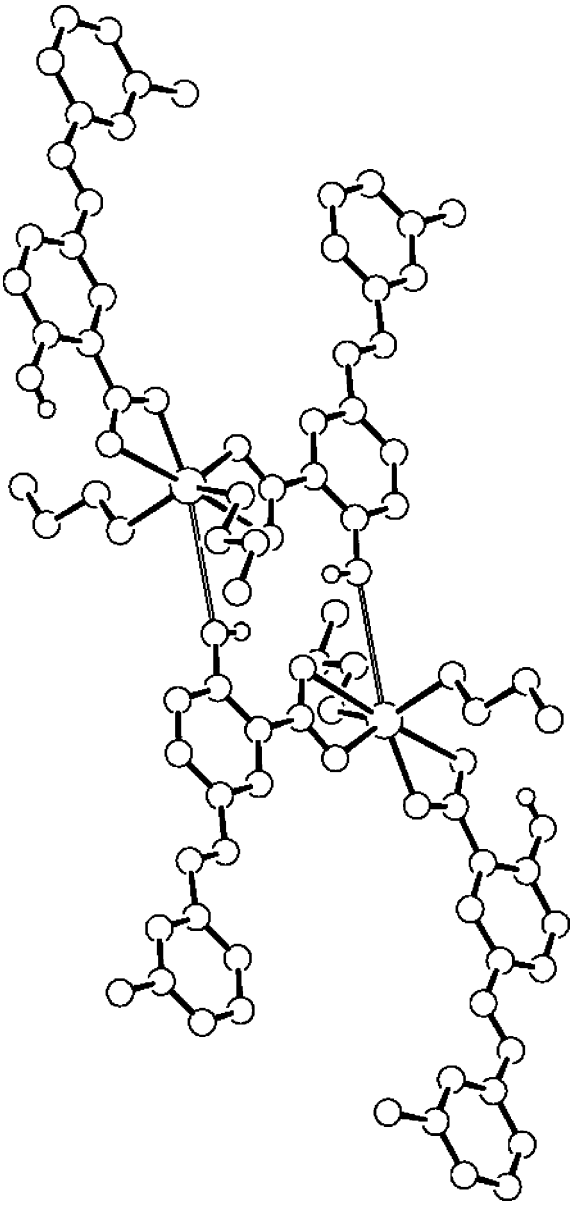

Fig. 7. The dimeric unit formed by the weak Sn···O interaction in **3**. Except for the hydroxy groups, the hydrogen atoms have been omitted for clarity.

the cationic part (Cat) of the molecule is measured in the positive-ion mode and the anionic part (An) in the negative-ion mode [17,18,32,33]. In all the $(LH)_2SnBu_2$ compounds, the bond between the Sn atom and the O atom from the carboxylate group is cleaved first. In addition to these ions, the $[M + Na]^+$ and $[M + K]^+$ ions are also observed in the positive-ion mode and the $[M–H]^-$ ions in the negative-ion mode in the ESI mass spectra. Some dimeric ions, such as $[2*Cat + Na]^+$ for **1** and **3** and $[2*Cat + K]^+$ for **1**, are observed as well. The presence and the relative abundances of these adducts with alkali metal ions depend mainly on the salt content in the samples. Compound **6** does not produce a signal in the positive-ion mode, unlike all of the other studied compounds. The compounds all display the deprotonated molecular ions $[M–H]^-$ which are the base peaks in the first-order negative-ion ESI mass spectra. In the negative-ion MS/MS spectra, the neutral loss of CO_2 (*m*/*z* 44) as a typical fragmentation path of carboxylic acids confirms the presence of a carboxylate group. The positive-ion MS/MS spectra are more complex and the following neutral losses are often found: butene, butane, C_6H_6, C_6H_4, CO_2, H_2O, the rearrangement loss of N_2 from the azo-group. All observed ions are in accordance with the expected structures.

3.4. Solution NMR

The ^1H and ^{13}C NMR data of the ligands are reported in [21,22]. The signals were assigned by the use of correlated spectroscopy (COSY), heteronuclear single-quantum correlation (HSQC) and Constant time Inverse-detection Gradient Accordion Rescaled (CIGAR) heteronuclear multiple-bond connectivities (HMBC) [34] experiments using gradient coherence selection. Rotating-frame Overhauser enhancement spectroscopy (ROESY) spectra were required in order to assign the aromatic protons adjacent to the methyl groups of ligands L^2HH' and L^3HH' due to overlapped B ring signals in the ^1H NMR spectra (in the case of L^2HH', the B ring ^1H signals were severely distorted due to very similar chemical shifts for H-3 and H-4). The conclusions drawn from the ligand assignments have subsequently been extrapolated to their Sn complexes owing to the similarity in the data. The ^1H and ^{13}C chemical shift assignments of the butyltin moiety are readily deducible from the multiplicity patterns and resonance intensities. The assignments of the signals for compounds **1**–**5** are reported elsewhere [20]. The solution ^{119}Sn NMR data (Table 3) in $CDCl_3$ solution are in the range −113 to −119 ppm and the values are consistent with those reported for $R_2Sn(O_2CR')_2$ systems [35–37].

3.5. ^{117}Sn Solid state NMR

The isotropic ^{117}Sn chemical shift and the data of the tensor analysis according to the method of Herzfeld and Berger [38] for compounds **1**–**6** are reported in Table 3. The isotropic chemical shifts are all in the range −93 to −114 ppm and are hardly different from the data in solution, implying the same coordination pattern, i.e. a trapezoidal bipyramid, is preserved. All compounds have almost axial symmetry (η ranging between 0.10 and 0.25). Compounds **2**–**4** have very similar σ_{11} and σ_{22}, the difference in σ_{33} being reflected in ζ and δ_{iso}. Compounds **5** and **6** are best compared with **1**: very similar values of η, ζ, σ_{22} and σ_{33} are observed, the effect of the substituent being felt only by σ_{11}. However, since the meaning of these parameters is not well documented, no conclusions can be drawn from these data. The weak

Table 3
Solution and solid state tin NMR data for compounds **1**–**6**

Compounds	δ ^{119}Sn ($CDCl_3$ solution)	^{117}Sn MAS[a]					
		δ_{iso}	ζ	η	σ_{11}	σ_{22}	σ_{33}
1	−114.6	−103	−645	0.20	285	156	−748
2	−113.8	−93[b]	−640	0.10	258	194	−733
3	−119.7	−114	−676	0.10	257	190	−790
4	−116.0	−100	−660	0.10	263	197	−760
5	−116.4	−95	−653	0.25	313	150	−748
6	−114.1	−100	−652	0.25	308	145	−752

[a] δ_{iso} (ppm) = $-\sigma_{iso} = -(\sigma_{11} + \sigma_{22} + \sigma_{33})/3$; ζ(ppm) = $\sigma_{33} - \sigma_{iso}$ and $\eta = |\sigma_{22} - \sigma_{11}|/|\sigma_{33} - \sigma_{iso}|$ where σ_{11}, σ_{22} and σ_{33} (ppm) are the principal tensor components of the chemical shielding anisotropy, sorted as follows $|\sigma_{33} - \sigma_{iso}| > |\sigma_{11} - \sigma_{iso}| > |\sigma_{22} - \sigma_{iso}|$.

[b] The solid state ^{117}Sn spectrum displays a second signal with $\delta_{iso} = -168$ ppm, with an intensity of about 1/3 of the major signal; after dissolution and evaporation of the sample this signal has disappeared.

Table 4
ID_{50} values (ng/ml) of test compounds in vitro used for the cell viability test

Test compound[a]	Cell lines						
	A498	EVSA-T	H226	IGROV	M19	MCF-7	WIDR
2	387	63	337	179	122	124	359
DOX	90	8	199	60	16	10	11
CPT	2253	422	3269	169	558	699	967
5-FU	143	475	340	297	442	750	225
MTX	37	5	2287	7	23	18	<3.2
ETO	1314	317	3934	580	505	2594	150
TAX	<3.2	<3.2	<3.2	<3.2	<3.2	<3.2	<3.2

[a] Abbreviations: **2** = $(L^2)H_2SnBu_2$, DOX = doxorubicin, CPT = cisplatin, 5-FU = 5-fluorouracil, MTX = methotrexate, ETO = etoposide and TAX = paclitaxel.

intermolecular interaction between the Sn atom and the hydroxy O atom of the 2-hydroxybenzoate of a neighbouring molecule, as seen in the crystal structures of compound **1** and **3**, is marginally reflected in the isotropic chemical shift of these compounds, being to lower frequency by 10–20 ppm when compared with the other derivatives. None of the solid state NMR parameters can be used as a useful indicator of coordination expansion by weak intermolecular Sn···O interactions. Compound **2** was not homogeneously crystalline. Its solid state ^{117}Sn spectrum contained, apart from the resonance at $\delta_{iso} = -93$ ppm, a second resonance at −168 ppm with an intensity of about one third of the former one. Since no contamination was detected in the solution spectrum of **2**, the lower frequency of the second resonance can only be ascribed to an additional minor crystal motif with a somewhat stronger intramolecular coordination between tin and the carboxylate oxygen atoms and/or a coordination extension at the tin atom arising from intermolecular aggregation of a different nature than the HO → Sn interaction proposed for compounds **1** and **3**. The exact nature of the minor species in **2** remains unclear.

3.6. In vitro cytotoxicity

Some diorganotin dicarboxylate compounds have shown quite promising antitumour activity [39,40]. The results of the in vitro cytotoxicity test of compound **2** against human tumour cell lines is given as ID_{50} values in Table 4, and compared with the data for some compounds that are in current clinical use as antitumour agents. The table clearly shows that compound **2** is more active in vitro than cisplatin and etoposide against all seven human cancer cell lines. This encouraging cytotoxic effect may be predictive of in vivo antitumour activity. Compound **2** may be a suitable candidate for modification in order to improve cytotoxic and dissolution properties.

4. Supplementary material

CCDC-238983–CCDC-238986 contain the supplementary crystallographic data for complexes **1**, **3**, **4**, and **6**, respectively. These data can be obtained free of charge via www.ccdc.cam.ac.uk/conts/retrieving.html (or from the Cambridge Crystallographic Data Centre, 12 Union Road, Cambridge CB2 1EZ, UK; fax: +44 1223 336033; e-mail: deposit@ccdc.cam.ac.uk).

Acknowledgements

The financial support of the Department of Science and Technology, New Delhi, India (Grant No. SP/S1/

F26/99, TSBB) and of the Czech Republic (Grant No. 203/03/1071, MH) are gratefully acknowledged. MB and RW are indebted to the Fund for Scientific Research Flanders, Belgium (FWO) for financial support (Grant No. 9.0016.02) as well as the Research Council of the VUB for matching funds.

References

[1] A.G. Davies, Organotin Chemistry, VCH, Weinheim, Germany, 1997.
[2] P.J. Smith, Chemistry of Tin, Blackie Academic & Professional, London, England, 1998.
[3] M.A. Champ, P.F. Seligman, Organotin. Environmental Fate and Effects, Chapman & Hall, London, England, 1996.
[4] (a) M. Gielen, Coord. Chem. Rev. 15 (1996) 41;
(b) S.J. Blunden, P.A. Cusack, R. Hill, Industrial Uses of Tin Chemicals, Royal Society of Chemistry, London, 1985;
(c) A.J. Crowe, in: M. Gielen (Ed.), Metal-Based Drugs, vol. 1, Freund Publishing House, London, 1989, pp. 103–149.
[5] C.J. Evans, S.J. Karpel, J. Organomet. Chem. Libr. 16 (1985) 1.
[6] T.P. Lockhart, J.C. Calabrese, F. Davidson, Organometallics 6 (1987) 2479.
[7] Y. Maeda, R. Okawara, J. Organomet. Chem. 10 (1967) 247.
[8] T.N. Mitchell, J. Organomet. Chem. 59 (1973) 189.
[9] S.G. Teoh, S.H. Ang, E.S. Looi, C.A. Keok, S.B. Teo, J.P. Declercq, J. Organomet. Chem. 523 (1996) 75.
[10] (a) E.R.T. Tiekink, Appl. Organomet. Chem. 5 (1991) 1;
(b) E.R.T. Tiekink, Trends Organomet. Chem. 1 (1994) 71.
[11] T.P. Lockhart, F. Davidson, Organometallics 6 (1987) 2471.
[12] R. Willem, I. Verbruggen, M. Gielen, M. Biesemans, B. Mahieu, T.S. Basu Baul, E.R.T. Tiekink, Organometallics 17 (1998) 5758.
[13] T.S. Basu Baul, E.R.T. Tiekink, Z. Kristallogr. 213 (1998) 62.
[14] T.S. Basu Baul, E.R.T. Tiekink, Z. Kristallogr. 214 (1999) 566.
[15] D. de Vos, R. Willem, M. Gielen, K.E. van Wingerden, K. Nooter, Metal-Based Drugs 5 (1998) 179.
[16] M. Nath, S. Pokharia, X. Song, G. Eng, M. Gielen, M. Kemmer, M. Biesemans, R. Willem, D. de Vos, Appl. Organometal. Chem. 17 (2003) 305.
[17] A. Rùžièka, L. Dostál, R. Jambor, V. Buchta, J. Brus, I. Ćísaøová, M. Holèapek, J. Holeèek, Appl. Organomet. Chem. 16 (2002) 315.
[18] A. Rùžièka, A. Lyèka, R. Jambor, P. Novák, I. Ćísaøová, M. Holèapek, M. Erben, J. Holeèek, Appl. Organomet. Chem. 17 (2003) 168.
[19] T.S. Basu Baul, S. Dhar, E.R.T. Tiekink, Main Group Met. Chem. 24 (2001) 293.
[20] T.S. Basu Baul, S. Dhar, E. Rivarola, F.E. Smith, R. Butcher, X. Song, M. McCain, G. Eng, Appl. Organomet. Chem. 17 (2003) 261.
[21] T.S. Basu Baul, S. Dhar, N. Kharbani, S.M. Pyke, R. Butcher, F.E. Smith, Main Group Met. Chem. 22 (1999) 413.
[22] T.S. Basu Baul, S. Dhar, S.M. Pyke, E.R.T. Tiekink, E. Rivarola, R. Butcher, F.E. Smith, J. Organomet. Chem. 633 (2001) 7.
[23] R. Hooft, *Kappa*CCD Collect Software, Nonius BV, Delft, The Netherlands, 1999.
[24] Z. Otwinowski, W. Minor, in: C.W. Carter, Jr., R.M. Sweet (Eds.), Methods in Enzymology, Macromolecular Crystallography, Part A, vol. 276, Academic Press, New York, 1997, pp. 307–326.
[25] R.H. Blessing, Acta Crystallogr., Sect. A 51 (1995) 33.
[26] A. Altomare, G. Cascarano, C. Giacovazzo, A. Guagliardi, M.C. Burla, G. Polidori, M. Camalli, SIR92, J. Appl. Crystallogr. 27 (1994) 435.
[27] P.T. Beurskens, G. Admiraal, G. Beurskens, W.P. Bosman, S. Garcia-Granda, R.O. Gould, J.M.M. Smits, C. Smykalla, PATTY: The DIRDIF Program System, Technical Report of the Crystallography Laboratory, University of Nijmegen, The Netherlands, 1992.
[28] P.T. Beurskens, G. Admiraal, G. Beurskens, W.P. Bosman, R. de Gelder, R. Israel, J.M.M. Smits, DIRDIF94: The DIRDIF Program System, Technical Report of the Crystallography Laboratory, University of Nijmegen, The Netherlands, 1994.
[29] G.M. Sheldrick, SHELXL97, Program for the Refinement of Crystal Structures, University of Göttingen, Germany, 1997.
[30] M.R. Boyd, Principles Practice Oncol. 3 (1989) 1.
[31] Y.P. Keepers, P.E. Pizao, G.J. Peters, J. Van Ark-Otte, B. Winograd, H.M. Pinedo, Eur. J. Cancer 27 (1991) 897.
[32] R. Jambor, L. Dostál, A. Rùžièka, I. Ćísaøová, J. Brus, M. Holèapek, J. Holeèek, Organometallics 21 (2002) 3996.
[33] L. Koláøová, M. Holèapek, R. Jambor, L. Dostál, A. Rùžièka, M. Nádvorník, J. Mass Spectrom. 39 (2004) 621.
[34] C.E. Hadden, G.E. Martin, V.V. Krishnamurthy, Magn. Reson. Chem. 38 (2000) 143.
[35] J. Otera, T. Hinoishi, Y. Kawabe, R. Okawara, Chem. Lett. (1981) 273.
[36] T.P. Lockhart, W.F. Manders, Inorg. Chem. 25 (1986) 892.
[37] T.P. Lockhart, Organometallics 7 (1988) 1438.
[38] J. Herzfeld, A.E. Berger, J. Chem. Phys. 73 (1980) 6021.
[39] A. Meriem, R. Willem, M. Biesemans, B. Mahieu, D. de Vos, P. Lelieveld, M. Gielen, Appl. Organomet. Chem. 5 (1991) 195.
[40] M. Gielen, M. Boualam, B. Mahieu, E.R.T. Tiekink, Appl. Organomet. Chem. 8 (1994) 19.